Environmental Science: Atmospheres

ROYAL SOCIETY OF CHEMISTRY

PAPER

View Article Online
View Journal | View Issue

Cite this: *Environ. Sci.: Atmos.*, 2023, **3**, 115

Effect of OH scavengers on the chemical composition of α-pinene secondary organic aerosol†

David M. Bell, *[a] Veronika Pospisilova,[ab] Felipe Lopez-Hilfiker,[ab] Amelie Bertrand,[a] Mao Xiao,[a] Xueqin Zhou,[a] Wei Huang, ‡[c] Dongyu S. Wang,[a] Chuan Ping Lee,[a] Josef Dommen,[a] Urs Baltensperger,[a] Andre S. H. Prevot,[a] Imad El Haddad[a] and Jay G. Slowik*[a]

OH scavengers are extensively used in studies of secondary organic aerosol (SOA) because they create an idealized environment where only a single oxidation pathway is occurring. Here, we present a detailed molecular characterization of SOA produced from α-pinene + O_3 with a variety of OH scavengers using the extractive electrospray time-of-flight mass spectrometer in our atmospheric simulation chamber, which is complemented by characterizing the gas phase composition in flow reactor experiments. Under our experimental conditions, radical chemistry largely controls the composition of SOA. Besides playing their desired role in suppressing the reaction of α-pinene with OH, OH scavengers alter the reaction pathways of radicals produced from α-pinene + O_3. This involves changing the HO_2 : RO_2 ratio, the identity of the RO_2 radicals present, and the RO_2 major sinks. As a result, the use of the OH scavengers has significant effects on the composition of SOA, including inclusions of scavenger molecules in SOA, the promotion of fragmentation reactions, and depletion of dimers formed *via* α-pinene RO_2–RO_2 reactions. To date fragmentation reactions and inclusion of OH scavenger products into secondary organic aerosol have not been reported in atmospheric simulation chamber studies. Therefore, care should be considered if and when to use an OH scavenger during experiments.

Received 16th August 2022
Accepted 1st November 2022

DOI: 10.1039/d2ea00105e

rsc.li/esatmospheres

Environmental significance

Secondary organic aerosol (SOA) is a major component of atmospheric particles, and is often simulated using laboratory studies in smog chambers. OH scavengers are a common additive to smog chambers, when reactions by other oxidants are investigated. OH scavengers are small organic molecules that possess too high volatility to contribute by themselves to formation of SOA. In this work, we demonstrate the impact of OH scavengers on the radical balance in smog chambers and its inclusion into SOA, which substantially alters SOA composition. This can have strong impacts on SOA yield parametrizations, volatility distribution determination and potentially the assessments of SOA toxicity and climate impacts. Therefore, the use of OH scavengers does not necessarily faithfully reproduce the processes occurring in the atmosphere.

1 Introduction

Organic aerosol (OA) makes up between 20–90% of the global aerosol burden.[1] Much of the OA in the atmosphere results from oxidation processes forming secondary species (secondary organic aerosol, SOA) that have low volatility, so after the transformation the formed molecules are more likely found in the particle phase than the gas phase.[2] Quantitative investigation of these processes in the atmosphere is often impractical due to the large number of precursor volatile organic compounds (VOCs) and possible reaction pathways. Therefore, comparison of ambient measurements to laboratory studies provides the opportunity to study single VOCs oxidized under controlled conditions, thus disentangling complexities present in the atmosphere.[3] Monoterpenes are prevalent VOC precursors and yield a substantial fraction of SOA globally, making them a frequent target for laboratory studies.[4]

Perhaps the most studied ideal system in the laboratory is the ozonolysis of α-pinene. Ozonolysis of alkenes also produces OH radicals with yields up to 115%,[5] providing a competing oxidation pathway which obscures the desired investigation of

[a]*Laboratory of Atmospheric Chemistry, Paul Scherrer Institute, 5232 Villigen, Switzerland. E-mail: david.bell@psi.ch; jay.slowik@psi.ch*

[b]*Tofwerk, 3600 Thun, Switzerland*

[c]*Institute of Meteorology and Climate Research, Karlsruhe Institute of Technology, 76344 Eggenstein-Leopoldshafen, Germany*

† Electronic supplementary information (ESI) available. See DOI: https://doi.org/10.1039/d2ea00105e

‡ Now at: Institute for Atmospheric and Earth System Research/Physics, Faculty of Science, University of Helsinki, 00014 Helsinki, Finland.

pure ozonolysis.[6] For example, during α-pinene ozonolysis experiments, up to half of the α-pinene is estimated to react with OH.[7] Therefore, the use of OH radical scavengers is standard practice to limit the oxidation to a single pathway and determine the corresponding yields of SOA formation,[7–12] physical properties,[13,14] and composition.[9,11,15–17] The yields of SOA formation have been extensively studied with scavengers and have been found to vary substantially based on the scavenger identity, where small molecules (*e.g.* methanol, formaldehyde, propanol) have lower yields of SOA formation than cyclohexane.[11] Overall, the use of a scavenger implicitly assumes that the scavenger exerts a negligible effect on SOA composition and properties.

By preventing the reaction of α-pinene with OH *via* an OH scavenger, a consequence is to limit the formation of OH oxidation products. While the reaction of α-pinene with O_3 mainly produces $C_{10}H_{15}O_{4,6}$ peroxy-radicals (RO_2), in reactions with OH radicals the main radicals formed are $C_{10}H_{17}O_{3,5}$.[18,19] Therefore, studies have reported the reduction of highly oxygenated molecules (HOMs) produced through the $C_{10}H_{17}O_x$ radical pathway, in the presence of an OH scavenger.[18,20] However, as an undesired effect, the use of an OH scavenger also alters the fate of the RO_2 radicals produced from ozonolysis and consequently the chemical composition of the resulting SOA. In the absence of nitrogen oxide (NO), RO_2 radicals react with HO_2 to form an alkoxy radical (RO) or hydroperoxides, or with other RO_2 radicals to form an RO radical or different closed shell molecules, including ROOR′ dimers (see ESI†).[19,21,22] The pathway to ROOR′ dimers is particularly important because these products have low volatility and are expected to be a major fraction of SOA.[19,23–25] Changes in RO_2 chemistry due to the use of scavengers alters the formation rates of dimers and the ability of RO_2 radicals to undergo autoxidation, and these effects on SOA composition require systematic evaluation. On the one hand, the presence of some OH scavengers (*e.g.* H_2, CO, alcohols, *etc.*) alters the $HO_2 : RO_2$ ratio,[10,11] which may have an effect on dimer yields. On the other hand, the identity of the RO_2 radicals formed will change because of the presence of a scavenger (*e.g.* cyclohexane, *etc.*), by replacing the RO_2 radicals formed from the α-pinene + OH pathway with the scavenger + OH oxidation pathway. The products of the reaction between two RO_2 radicals are strongly dependent on the radical structure, where the reaction branching ratios are in favor of dimer formation for larger radicals.[18,19,21,26,27] Therefore, while RO_2 radicals formed from small scavengers are expected to decrease dimer formation, radicals from larger scavengers are expected to recombine with the radicals from the VOC of interest forming mixed dimers. The latter have been observed in flow tube reactors[18,26] and in the gas phase in smog chamber studies,[27] but particle phase observations are currently lacking. Accordingly, OH scavengers can affect many aspects of the oxidation process, and their ubiquitous use in the atmospheric community necessitates the study of their effects on SOA formation and its composition.

Here, we explore the chemical changes in α-pinene SOA forming in the presence and absence of different OH scavengers (butanol, cyclopentane, and cyclohexane). We utilize the extractive electrospray ionization time-of-flight mass spectrometer (EESI-TOF),[28] as a soft ionization technique, to probe the changes on a molecular level. To understand the gas phase reactions leading to the observed molecules in the particle phase, we complement the SOA studies by also using a flow reactor.

2 Experimental

Studies were performed in Teflon atmospheric simulation chambers (27 m^3 or 8 m^3) at the Paul Scherrer Institute.[29,30] The chambers are housed in temperature-controlled enclosures maintained at 20 ± 1 °C. The relative humidity (RH) for each experiment was 50%. Instrumentation included a proton-transfer mass spectrometer (PTR-MS, PTR-TOF-8000, Ionicon), an EESI-TOF including an atmospheric pressure time-of-flight mass spectrometer (Tofwerk), a scanning mobility particle sizer (SMPS, TSI model 3938) and an ozone gas monitor (Thermo 49C). Experiments were performed by injecting ozone into the chamber (200–500 ppb), followed by injection of an OH scavenger (if used), and then α-pinene (see Table S1† for details). Gas phase concentrations were monitored by a PTR-MS and for selected experiments a NO_3-chemical ionization mass spectrometer (NO_3-CIMS). The OH scavengers utilized were *n*-butanol (~100 ppm), cyclopentane (200 ppm), and cyclohexane (200 ppm). These concentrations of OH scavenger resulted in OH reacting with the scavenger 99.9% of the time for all scavengers. The EESI-TOF provides highly time-resolved measurements (1 Hz) of the SOA molecular ions. The aerosol flow is continuously sampled and intersects with a spray of charged droplets doped with ~100 ppm of NaI generated by a conventional fused silica electrospray capillary. The water-soluble portion of the aerosol is extracted into the droplets, which then yields intact SOA molecules in the form of Na^+-adducts. Prior to interaction with the electrospray, a multi-walled charcoal denuder strips the gas phase constituents and leaves the aerosol, alone, to interact with the electrospray. The aerosol sample was regularly switched to a filter blank (4 min sample and 1 min filter) throughout the experiment to obtain regular background measurements. Detailed descriptions of the instrument can be found in lab studies,[28,31] as well as in field studies.[32,33] The particle phase mass concentrations were calculated using the size distributions obtained by the SMPS using a density of 1.2 g cm^{-3}.[34] The maximum mass concentrations are reported in Table 1 and are between 23–28 μg m^{-3} when no scavenger is present. The mass loadings are 12–16 μg m^{-3} when OH scavengers are used, similar to the reductions observed in Iinuma *et al.*[9]

Flow-tube experiments were also performed in a ~5 L glass vessel with a total flow rate of 20 L min^{-1}, resulting in a residence time of ~12 seconds at an RH of ~5%. A constant source of α-pinene and ozone was injected into the flow tube, periodically an OH scavenger was additionally injected into the flow tube while maintaining a constant flow rate (see Table 1 for conditions). A condensation particle counter (CPC, TSI 3776, lower cut off 2.5 nm) continually monitored the particle number concentration and showed no particle formation in any experiment. During the flow-tube experiments the multi-channel denuder was removed from the EESI-TOF and the direct gas-

Table 1 Experimental conditions explored with the flow tube and atmospheric simulation chamber

Experiment #	Scavenger	Experimental setup	α-Pinene (ppb)	Scavenger (ppm)	O_3 (ppb)	Mass loading (μg m^{-3})
1	No	Smog chamber	25	—	160	23
2	No	Smog chamber	25	—	225	28
3	No	Flow tube	10	—	5000	—
4	Butanol	Smog chamber	25	200	250	16
5	Butanol	Flow tube	10	200	5000	—
6	Cyclohexane	Smog chamber	25	200	230	15
7	Cyclohexane	Flow tube	10	200	5000	—
8	Cyclopentane	Smog chamber	25	200	200	12

phase products were detected. Backgrounds were assessed by comparing the signal observed by the EESI-TOF when only zero air was being passed through the flow tube both before and after each experiment, to achieve background levels. As mentioned above the total flow rate of the flow tube was 20 L min^{-1} and the flow rate from the flow tube to the EESI-TOF (~0.5 m) was 10 L min^{-1}, while the EESI-TOF sampled at 1 L min^{-1} *via* a 3 cm long stainless steel tube. Below, the flow tube data is used to explore relative changes in the composition, and to verify products that are formed in the gas phase resulting from interactions between OH scavengers and α-pinene oxidation products. Therefore, absolute concentrations and reaction rates were not obtained. The experiments here were modelled with a 0-D box model (F0AM)[35] using the chemical mechanism in MCM 3.3.1.[36,37]

3.1 Experimental results

Previous work performed in our chambers utilizing α-pinene SOA, in Pospisilova *et al.*, showed the composition of α-pinene to be highly time-dependent, and products from OH chemistry ($C_{10}H_{18}O_x$ molecules) were found to be especially reactive with lifetimes below 30 minutes.[31] Due to the complex evolution in composition, we will initially discuss EESI-TOF composition measurements performed at two experimental times: (1) within the first 30 minutes of the experiment; and (2) at the maximum of SOA mass. Fig. 1A–D show the carbon distribution at maximum mass with the bars colored by the number of oxygen atoms present for experiments without an OH scavenger, and with butanol, cyclopentane, and cyclohexane as OH scavengers. Fig. 1A shows the typical composition of α-pinene SOA formed without a scavenger at the time of maximum mass, binned in terms of the number of C and O atoms (*x*-axis and colors, respectively). Overall, C_5–C_{10} molecules dominate in the monomer region and C_{14}–C_{20} molecules in the dimer region, which together represent more than 90% of the total EESI-TOF signal observed in all scavenger-free experiments. The largest fraction of molecules formed contains 10 carbon atoms, and the hydrogen distribution for the C_{10} species consists mainly of H =

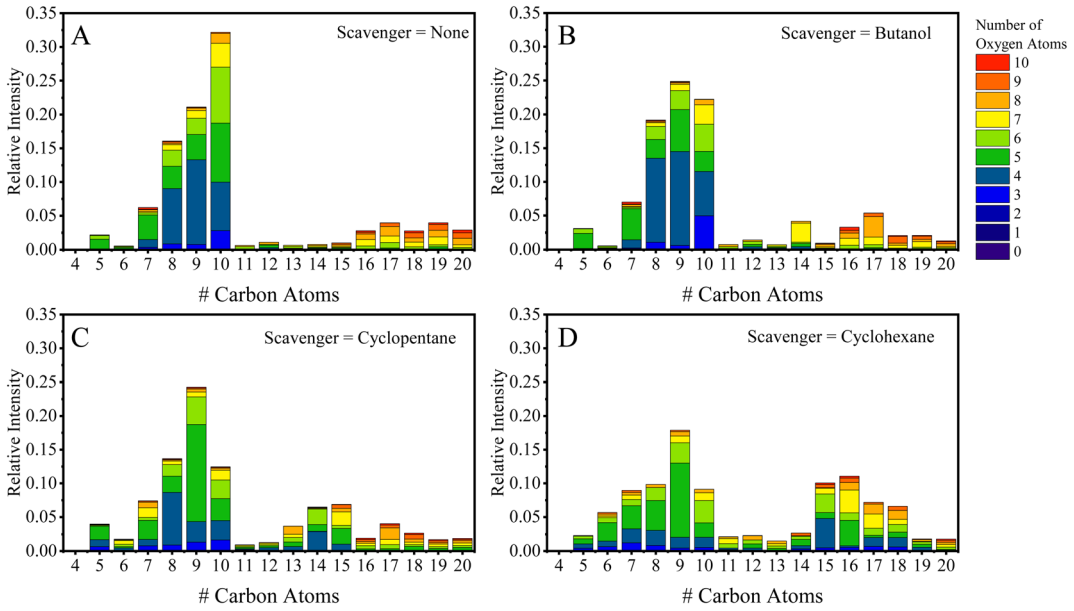

Fig. 1 (A–D) Data from EESI-TOF binned according to number of carbon atoms (*x*-axis) and number of oxygen atoms at the time of maximum SOA mass concentration during an α-pinene ozonolysis experiment with (A) no scavenger present, (B) butanol present, (C) cyclopentane present, and (D) cyclohexane present.

14, 16, and 18. Previous work shows it is possible to separate the contribution of different oxidation schemes (OH *vs.* O_3) (*e.g.*, $C_{10}H_{14}O_x$ and $C_{10}H_{16}O_x$ are formed from O_3 chemistry, while $C_{10}H_{16}O_x$ and $C_{10}H_{18}O_x$ come from OH chemistry).[18,19] Therefore, the $C_{10}H_{18}O_x$ molecules can be used as an initial assessment for whether or not the OH chemistry pathway is depleted.

Fig. 2A and B break down the C_{10} species observed by the EESI-TOF in terms of number of hydrogen atoms (H = 12, 14, 16, and 18) with number of oxygen atoms between 2–10 in experiments without an OH scavenger and butanol as an OH scavenger, respectively, 30 min after the addition of α-pinene. The $C_{10}H_{18}O_x$ fraction without the scavenger is ~25% of the total C_{10} contribution, consisting of O_4–O_7 molecules (Fig. 2A), while the butanol scavenger $C_{10}H_{18}O_x$ fraction is only ~15% (Fig. 2B). Overall, the fraction of $C_{10}H_{18}O_x$ is significantly reduced for the latter case, and instead of spanning #O = 4–7, $C_{10}H_{18}O_4$ is almost exclusively formed. $C_{10}H_{18}O_4$ was found previously to decay away quickly in the particle phase, likely due to its high reactivity.[31] While the majority of $C_{10}H_{18}O_x$ molecules are formed through OH chemistry, $C_{10}H_{18}O_4$ can also be formed *via* the reaction of the Criegee intermediate with H_2O.[15,19] Additionally, the change associated with the scavenger demonstrates that the $C_{10}H_{18}O_x$ molecules (x = 5–7) are not a result of water clusters with $C_{10}H_{16}O_x$ molecules, but rather formed *via* OH chemistry. Results when using cyclohexane as a scavenger are included in the ESI (Fig. S1A†), and agree with the results shown in Fig. 2, while formation of dimers *via* cyclopentane oxidation products complicates the analysis for that system (Fig. S1B†).

Fig. 1B–D show the carbon distribution at maximum mass when butanol (1B), cyclopentane (1C), and cyclohexane (1D) were used as OH scavengers. Comparing Fig. 1A (no scavenger) to 1B (butanol scavenger), there is depletion of the C_{10} molecules relative to the C_9 molecules, which will be discussed further below. In the dimer region, the fraction of the C_{19}–C_{20} molecules decreases from 6.8% (without scavenger) to 3.0% (with butanol). The $C_{20}H_{30-34}O_x$ fraction measured by the NO_3^--CIMS is depleted (Fig. S2C and D†), which is consistent with previous flow tube studies[18] and the particle phase composition (Fig. S3†). The C_{16}–C_{18} region observes small changes on a relative scale (see Table S1†). Though, considering the mass concentration is lower for the scavenger experiments, the butanol and cyclopentane experiments exhibit lower absolute concentrations of C_{16-18} dimers, while the cyclohexane experiments have no difference relative to the no-scavenger experiment (excluding the mixed dimer products). The depletion of dimers comes from a change in the RO_2 identities. For instance C_{14} molecules are not observed in the reaction without scavengers, while C_{14} molecules form *via* reactions between butanol radicals and α-pinene radicals. The main RO_2 radical from the butanol scavenger is $C_4H_9O_3$.[10,18,26,37,38] $C_4H_9O_3$ then reacts with the RO_2 radicals from α-pinene ozonolysis, $C_{10}H_{15}O_{4,6}$, to form the dominant C_{14} mixed dimers observed ($C_{14}H_{24}O_{5,7}$) with an odd number of oxygen atoms. Another possibility to form C_{14} dimers could come from the reaction between the stabilized Criegee intermediate and the scavenger directly (*i.e.* $C_{10}H_{16}O_3$ + $C_4H_{10}O$),[17,39] the products of which would form $C_{14}H_{26}O_4$. Based on the concentrations of the butanol and water in the chamber, approximately half of the reactivity of the Criegee should take place with butanol (assuming a reaction rate similar to propanol).[40] However, $C_{14}H_{26}O_4$ makes up less than 0.01% of the total EESI-TOF signal in the chamber, suggesting this pathway is not significant under our experimental conditions, or the species is too volatile to be in the particle phase. Overall, the formation of C_{14} molecules is a clear indicator that there exist unwanted effects of using scavengers on the chemistry occurring in the chamber.

Fig. 1C and D show that the 'mixed dimers' formed from the cycloalkane experiments are $C_{16}H_{26}O_{5,7}$ and $C_{15}H_{24}O_{5,7}$ for the cyclohexane and cyclopentane experiments, respectively, and preferentially form with odd-numbered oxygen atoms. If the formation pathway is the same as for butanol, then the molecules with an odd number of oxygen atoms must come from the mixture of an RO_2 with even number of oxygen atoms + RO_2 with odd number of oxygen atoms. The dominant α-pinene RO_2 radicals are $C_{10}H_{15}O_{4,6}$ and they must combine with either

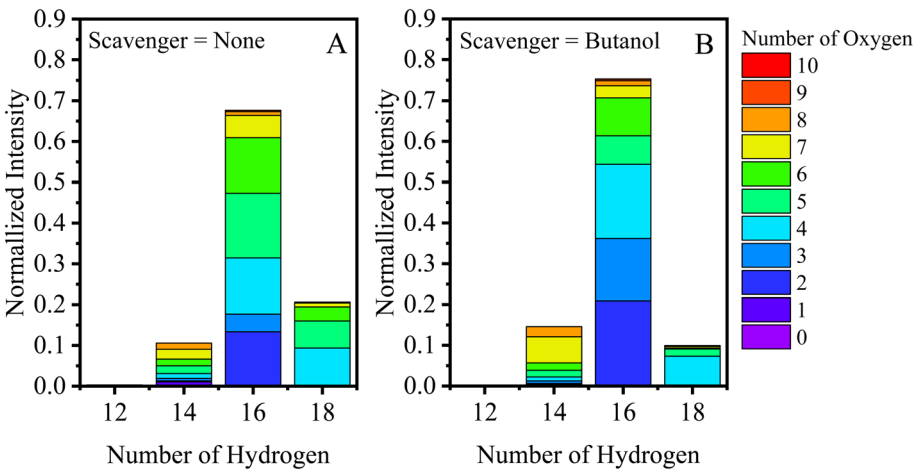

Fig. 2 Hydrogen distribution plotted for $C_{10}H_xO_y$ molecules (30 min after α-pinene addition), and colored according to the number of oxygen atoms present for an experiment (A) without an OH scavenger, and (B) with butanol present as a scavenger.

$C_6H_{11}O_3$ or $C_5H_9O_3$, respectively, to form the formula shown above. These formulae differ from the initial scavenger RO_2 formed from the reaction with an OH radical, which are $C_6H_{11}O_2$ (cyclohexane) and $C_5H_9O_2$ (cyclopentane).[41] Reaction schemes in the ESI (Schemes S1 and S2†) show how the initial RO_2 can react with another RO_2 to form an alkoxy radical, which can rapidly undergo a ring-opening reaction to form a second generation RO_2 radical. These second-generation RO_2 radicals ($C_6H_{11}O_3$ – cyclohexane and $C_5H_{11}O_3$ – cyclopentane) possess a formula matching the expected combination of scavenger and α-pinene oxidation products. An additional aspect in these experiments comes from the formation of dimers that have a carbon number equal to: $C_{scav} + C_{10} - 1$, which forms $C_{15}H_{24}O_{4,6}$ in the cyclohexane experiment. In addition, there appears to be a systematic decrease in the C_{10} species with the increasing carbon content of the OH scavenger. For example, the C_{10} fraction decreases from 32% (no scavenger) to 23% (butanol), 12% (cyclopentane), and 9% (cyclohexane), which cannot be explained by changes in mass concentrations. Considering the scavenging of OH is effectively the same in all experiments (with scavengers) and the mass concentrations are similar, the observed differences should be attributed to radical reactions between the oxidation products of the scavengers and α-pinene. One possibility is that the reactions with RO_2 radicals from cycloalkanes promote reactions *via* the alkoxy pathway which undergo subsequent fragmentation reactions. The cycloalkane experiments also exhibit the formation and inclusion of a small fraction of scavenger dimers (C_{12} – cyclohexane: see Fig. 1D, and C_{10} – cyclopentane: see Fig. S1B†), and small amounts of scavenger oxidation products (Fig. 1C and D), demonstrating three pathways for scavenger inclusions into SOA.

We further designed a flow-tube experiment to investigate the formation of the 'mixed dimers' in the gas phase from the systems discussed so far. The bar plot of Fig. 3 shows the gas-phase EESI-TOF signal (with scavenger)/EESI-TOF signal (without scavenger) for experiments with butanol and cyclohexane, with a CPC verifying particle number concentration <1 cm^{-3}. The ESI (Fig. S4†) includes a time series to demonstrate how the injection of a scavenger influences the gaseous oxidation products in real-time. As we can see from Fig. 3, depletion of C_{10} molecules formed *via* OH chemistry are observed, with $C_{10}H_{16}O_x$ depleted by 10–20%, and $C_{10}H_{18}O_x$ depleted by up to 60% which is less than the depletion (80–90%) observed in the chamber experiment (Fig. 2). This could result from incomplete mixing in the flow tube, and does not result from changes in gas-particle partitioning due to the lower mass loadings with scavengers (presented in the ESI†). Unfortunately, the small signal-to-noise ratio for the $C_{10}H_{18}O_x$ molecules results in relatively large error bars. Depletion of C_{20} dimers occurs with the addition of a scavenger, with $C_{20}H_{32}O_x$ being depleted by 90% and exhibiting an even–odd oxygen atom behavior. Dimers with odd number of oxygen atoms are depleted because these molecules are formed from RO_2–RO_2 reactions of the OH ($C_{10}H_{17}O_{3,5}$) and O_3 reaction pathways ($C_{10}H_{15}O_{4,6}$). $C_{20}H_{30}O_{5,7}$ molecules are also depleted by up to 80%, while the rest of the $C_{20}H_{30}O_x$ are only slightly diminished (by 30–50%), consistent with.[18]

For the experiments with a butanol scavenger, the main 'mixed dimers' formed have an odd number of oxygen atoms ($C_{14}H_{24}O_{5,7,9,11}$), in good agreement with results from the smog chamber experiments, discussed above. In contrast, there is a difference between flow tube and the smog chamber results for the cyclohexane experiments where the principal number of oxygen atoms for the $C_{16}H_{26}O_x$ 'mixed dimers' in Fig. 3 are even $C_{16}H_{26}O_{4,6,8}$, which differs from the results from the smog chamber (odd) in Fig. 1D ($C_{16}H_{26}O_5$ and O_7). When modelling the oxidation processes with the 0-D box model (F0AM) from the flow tube and the smog chamber, the ratio of the $C_6H_{11}O_2$: $C_6H_{11}O_3$ varies substantially between the two experiments (~20 for smog chamber and 100–300 in the flow tube). The difference in the ratio comes from the time scale of the two experiments, and is not impacted by the concentration difference in the experiments. The initial RO_2 radicals are still being formed in the flow tube, while longer times in the smog chamber allows the RO_2 radicals to undergo further reactions (with other RO_2 or HO_2 radicals) forming second- and third-generation radicals. Therefore, differences in the 'mixed dimer' formed in the flow

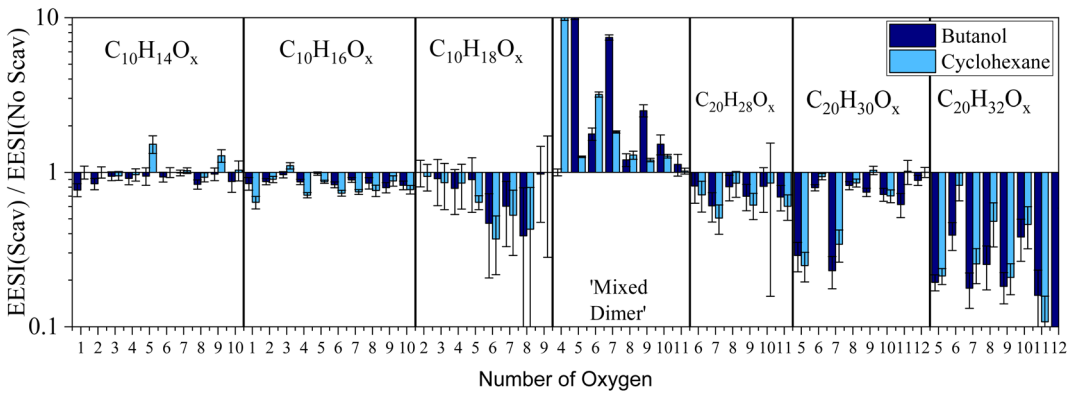

Fig. 3 Ratio of gas-phase EESI-TOF signals with scavenger to gas-phase EESI-TOF signal without scavenger observed from the flow tube for specific molecular classes. Mixed dimer contribution is shown as absolute intensity scaled so the maximum intensity is 10 from each experiment. The mixed dimer class corresponds to the $C_{14}H_{24}O_x$ (butanol) and $C_{16}H_{26}O_x$ (cyclohexane).

tube (O_4 and O_6) *vs.* the smog chamber (O_5 and O_7) reflect the distribution of the scavenger RO_2 radicals present. Because the main 'mixed dimer' formed in the chamber comes from the second-generation scavenger RO_2 radical ($C_6H_{11}O_3$) despite the initial scavenger RO_2 ($C_6H_{11}O_2$) having a larger concentration demonstrates mixed dimer formation is faster between α-pinene-RO_2 radicals and $C_6H_{11}O_3$ when compared to $C_6H_{11}O_2$. This is in agreement with the fact that dimer formation rates increase with the increase of the RO_2 oxygen content.[42,43]

In addition, the extent of C_{10} depletion differs depending on the identity of the scavenger in both the smog chamber (Fig. 1) and flow tube (Fig. 3). When considering the RO_2 reaction pathways for each scavenger (shown in the ESI†), the fates of the RO_2 radicals down the alkoxy pathway lead to different results. The butanol derived alkoxy radical terminates with the formation of HO_2 and acetaldehyde. Scheme S1† shows the cyclohexane RO_2 radicals going through an alkoxy radical until terminating with an HO_2 radical. A consequence of the alkoxy pathway can be an enhancement of unimolecular fragmentation products,[19] resulting in a shift in the carbon distribution away from C_{10} molecules to smaller carbon containing species (C_{7-9}). Consequently, there is a shift in the carbon distribution toward smaller carbon containing molecules for all scavengers used in the chamber (Fig. 1) with the most substantial depletion occurring for the cycloalkanes in particular, which supports this explanation.

3.2 Modelling and discussion

Some of the changes observed from the use of scavengers comes from changes in the radical balance that occurs. Fig. S4† highlights the reactivity of α-pinene-RO_2 with HO_2, and RO_2 radicals from either the scavenger or α-pinene, assuming general rates of RO_2 + RO_2 and RO_2 + HO_2 currently used in MCM 3.3.1. These results highlight the importance of HO_2 in the butanol experiment because of the pathway to form butanal + HO_2, which promotes RO_2 radical termination to ROOH monomers over dimer formation. The dimer fraction in Table S1† (and Fig. 1) is roughly similar for all experiments, though the difference in mass loading between experiments will result in a change in the absolute concentration of the dimers. If the EESI results are presented in terms of the total mass flux of the EESI (attograms per second obtained by # s^{-1} × MW × 1 × 10^{18}/Avogadro's number) the total dimer signal (C_{14-20}) for the no scavenger experiment (4 ag s^{-1}) is greater than the absolute dimer signal (2.7 ag s^{-1}), consistent with the greater importance of RO_2 + HO_2. For the cycloalkane experiments, the absolute concentration of the dimer range (C_{14-20}) is not dramatically different to the no-scavenger experiment (cyclopentane – 3.5 ag s^{-1}, cyclohexane – 4.2 ag s^{-1}), consistent with the importance of RO_2 + RO_2 dimer formation on SOA formation. Though, a systematic study on the rates of the RO_2 + RO_2 reactions and their branching ratios using a flow reactor would be needed to validate any quantitative modelling of these systems.

Our results raise questions about previous studies that have used OH scavengers to examine SOA physical properties or chemical composition. It also raises the question: why have these products not been previously observed in SOA? Previous measurements of SOA formed in the presence of a scavenger have generally used techniques with harsh ionization processes with substantial fragmentation,[17,34] or investigations of these molecules have not been a priority when employing offline techniques. Filter sampling techniques can also introduce artefacts and time that affords reactive species to degrade prior to analysis, as has been shown for reactive oxygen species from filter analysis.[44] Therefore, filter extracts that have measured the chemical composition of SOA may not be an effective method for measuring potentially reactive species formed *via* RO_2–RO_2 reactions, including species that hydrolyze in the presence of water or other solvents.

Further, these results show the use of scavengers that form RO_2 radicals is problematic because it can result in the incorporation of unwanted species into SOA (*e.g.* mixed dimers and scavenger oxidation products), as well as creating a radical environment that dramatically changes the monomer composition of SOA. Without accounting for sensitivity differences of different molecules measured by the EESI-TOF and using purely the relative intensities, shown in Fig. 1, the scavenger incorporated into SOA reaches nearly 20% for cyclohexane, while for the other scavengers the total fraction of artefacts decreases with decreasing carbon number of the scavenger (shown in Table S1†), down to ~7% for butanol. This accounting includes the increase in C_6 molecules for the cyclohexane experiment (see Fig. 1A *vs.* 1D) originating from inclusions of cyclohexane oxidation products. Similar increases are also observed in C_{12} molecules and the 'mixed dimers' (Fig. 1D). The change in the radical pathways and the incorporation of unwanted scavenger oxidation products in α-pinene SOA demonstrates the necessity to consider which OH scavenger to use and if to use an OH scavenger at all. Additionally, the atmosphere is rife with potential scavengers of OH radicals, and ultimately scavengers used within chambers should effectively mimic atmospheric conditions. Currently, many chamber experiments possess large concentrations of RO_2 radicals, while in the atmosphere HO_2 is a significant sink of RO_2 radicals. Therefore, the goal should be to use scavengers that do not incorporate the scavenger and that produce an atmospherically relevant radical balance (*e.g.* HO_2 *vs.* RO_2).

Scavengers such as H_2, CO, and H_2O_2 are good candidates because they will only produce HO_2 radicals, but the drawbacks of these scavengers include the large concentrations required (H_2 – 2%), potential safety hazards (H_2 and CO), and the uptake into the particle phase at elevated RH (H_2O_2). To probe the impact of the HO_2 : RO_2 ratio from different scavengers, a simple chamber box model using MCM[37,38] simulated the RO_2 : HO_2 ratio in the chamber in Fig. 4 (the absolute concentrations are shown in Fig. S5†). For comparison, Fig. 4 also includes other scavengers such as, CO, H_2, H_2O_2, and a series of alcohols, to probe the differences between RO_2 and HO_2 concentrations. RO_2 concentrations are always at least one order of magnitude greater than the HO_2 concentrations for all conditions explored here. Despite the large concentrations of RO_2 radicals, the reaction rate between HO_2–RO_2 is ~2 orders of magnitude faster than RO_2–RO_2 reactions, consequently HO_2–

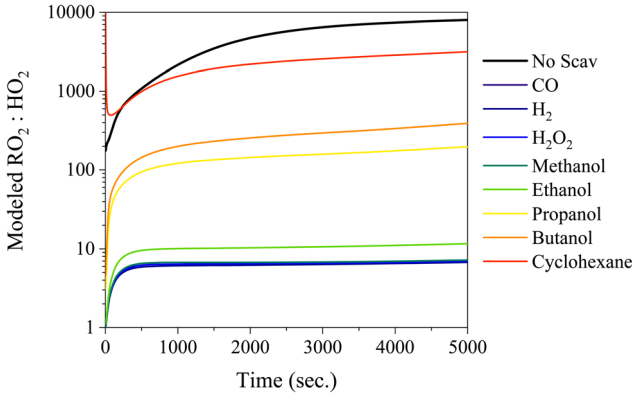

Fig. 4 RO_2 : HO_2 ratio modelled using a box model based on MCM v3.3.1 for: α-pinene 25 ppb, O_3 250 ppb, and excess concentration of the scavenger (CO – 30 000 ppm, H_2 – 2%, H_2O_2 – 200 ppm, methanol – 200 ppm, ethanol – 200 ppm, *n*-propanol – 200 ppm, *n*-butanol – 200 ppm, and cyclohexane – 200 ppm).

RO_2 will be the dominant reaction pathway when the RO_2 : HO_2 is below 100 (*e.g.* CO, H_2O_2, H_2, methanol, and ethanol). Reactions between HO_2 and RO_2 will also promote the formation of peroxide functional groups and inhibit formation of dimers *via* the RO_2–RO_2 pathway. Additionally, higher concentrations of HO_2 more realistically capture the HO_2 : RO_2 ratio present in the atmosphere as opposed to the RO_2 dominant chemistry regime typically found in chambers.

In summary, the roles of the scavengers in these experiments are multi-faceted because they influence the HO_2 : RO_2 ratio, the identity of the RO_2 radicals present, and the fate of the RO_2 radicals. The differences in the types of radicals produced in the gas phase (OH *vs.* HO_2 *vs.* scavenger-RO_2 *vs.* α-pinene-RO_2) ultimately determines a substantial fraction of the composition of the SOA formed. Given many fundamental studies about SOA are performed in chambers or flow tubes with the presence of a scavenger, it is important to understand the role they will play in the chemistry taking place. This study shows significant changes in composition of α-pinene SOA as a function of OH scavenger and necessitates their further study and consideration.

Data availability

Data can be found at the Eurochamp Database of Atmospheric Simulation Chamber Studies (**https://data.eurochamp.org/**).

Author contributions

Chamber investigations were performed by DB, VP, FL, AB, MX, XZ, and WH. Flow tube studies were investigated by DB, DSW, CPL. JS, AP, IEH and UB obtained funding for this work. DB prepared the manuscript with contributions from all co-authors.

Conflicts of interest

The authors declare no conflict of interests with the performed work.

Acknowledgements

This work was supported by the Swiss National Science Foundation (starting grant BSSGI0_155846, grant 200020_172602, grant 200021_169787) as well as the European Union's Horizon 2020 Research and Innovation Program through the EUROCHAMP-2020 Infrastructure Activity under grant agreement no. 730997. We would also like to thank Rene Richter for his assistance in installing and assembling the experimental setup.

References

1 J. L. Jimenez, M. R. Canagaratna, N. M. Donahue, A. S. Prevot, Q. Zhang, J. H. Kroll, P. F. DeCarlo, J. D. Allan, H. Coe, N. L. Ng, A. C. Aiken, K. S. Docherty, I. M. Ulbrich, A. P. Grieshop, A. L. Robinson, J. Duplissy, J. D. Smith, K. R. Wilson, V. A. Lanz, C. Hueglin, Y. L. Sun, J. Tian, A. Laaksonen, T. Raatikainen, J. Rautiainen, P. Vaattovaara, M. Ehn, M. Kulmala, J. M. Tomlinson, D. R. Collins, M. J. Cubison, E. J. Dunlea, J. A. Huffman, T. B. Onasch, M. R. Alfarra, P. I. Williams, K. Bower, Y. Kondo, J. Schneider, F. Drewnick, S. Borrmann, S. Weimer, K. Demerjian, D. Salcedo, L. Cottrell, R. Griffin, A. Takami, T. Miyoshi, S. Hatakeyama, A. Shimono, J. Y. Sun, Y. M. Zhang, K. Dzepina, J. R. Kimmel, D. Sueper, J. T. Jayne, S. C. Herndon, A. M. Trimborn, L. R. Williams, E. C. Wood, A. M. Middlebrook, C. E. Kolb, U. Baltensperger and D. R. Worsnop, Evolution of organic aerosols in the atmosphere, *Science*, 2009, **326**, 1525–1529.

2 M. Hallquist, J. C. Wenger, U. Baltensperger, Y. Rudich, D. Simpson, M. Claeys, J. Dommen, N. M. Donahue, C. George, A. H. Goldstein, J. F. Hamilton, H. Herrmann, T. Hoffmann, Y. Iinuma, M. Jang, M. E. Jenkin, J. L. Jimenez, A. Kiendler-Scharr, W. Maenhaut, G. McFiggans, T. F. Mentel, A. Monod, A. S. H. Prévôt, J. H. Seinfeld, J. D. Surratt, R. Szmigielski and J. Wildt, The formation, properties and impact of secondary organic aerosol: current and emerging issues, *Atmos. Chem. Phys.*, 2009, **9**, 5155–5236.

3 M. Riva, L. Heikkinen, D. M. Bell, O. Peräkylä, Q. Zha, S. Schallhart, M. P. Rissanen, D. Imre, T. Petäjä, J. A. Thornton, A. Zelenyuk and M. Ehn, Chemical transformations in monoterpene-derived organic aerosol enhanced by inorganic composition, *npj Clim. Atmos. Sci.*, 2019, **2**, 2.

4 H. Zhang, L. D. Yee, B. H. Lee, M. P. Curtis, D. R. Worton, G. Isaacman-VanWertz, J. H. Offenberg, M. Lewandowski, T. E. Kleindienst, M. R. Beaver, A. L. Holder, W. A. Lonneman, K. S. Docherty, M. Jaoui, H. O. T. Pye, W. Hu, D. A. Day, P. Campuzano-Jost, J. L. Jimenez, H. Guo, R. J. Weber, J. de Gouw, A. R. Koss, E. S. Edgerton, W. Brune, C. Mohr, F. D. Lopez-Hilfiker, A. Lutz, N. M. Kreisberg, S. R. Spielman, S. V. Hering, K. R. Wilson, J. A. Thornton and A. H. Goldstein, Monoterpenes are the largest source of summertime organic aerosol in the

southeastern United States, *Proc. Natl. Acad. Sci. U. S. A.*, 2018, **115**, 2038.

5 A. R. Rickard, D. Johnson, C. D. McGill and G. Marston, OH Yields in the Gas-Phase Reactions of Ozone with Alkenes, *J. Phys. Chem. A*, 1999, **103**, 7656–7664.

6 R. Atkinson, S. M. Aschmann, J. Arey and B. Shorees, Formation of OH radicals in the gas phase reactions of O3 with a series of terpenes, *J. Geophys. Res.: Atmos.*, 1992, **97**, 6065–6073.

7 K. M. Henry and N. M. Donahue, Effect of the OH Radical Scavenger Hydrogen Peroxide on Secondary Organic Aerosol Formation from α-Pinene Ozonolysis, *Aerosol Sci. Technol.*, 2011, **45**, 696–700.

8 N. M. Donahue, K. E. Huff Hartz, B. Chuong, A. A. Presto, C. O. Stanier, T. Rosenhørn, A. L. Robinson and S. N. Pandis, Critical factors determining the variation in SOA yields from terpene ozonolysis: A combined experimental and computational study, *Faraday Discuss.*, 2005, **130**, 295–309.

9 Y. Iinuma, O. Böge, Y. Miao, B. Sierau, T. Gnauk and H. Herrmann, Laboratory studies on secondary organic aerosol formation from terpenes, *Faraday Discuss.*, 2005, **130**, 279–294.

10 M. D. Keywood, J. H. Kroll, V. Varutbangkul, R. Bahreini, R. C. Flagan and J. H. Seinfeld, Secondary Organic Aerosol Formation from Cyclohexene Ozonolysis: Effect of OH Scavenger and the Role of Radical Chemistry, *Environ. Sci. Technol.*, 2004, **38**, 3343–3350.

11 K. S. Docherty and P. J. Ziemann, Effects of Stabilized Criegee Intermediate and OH Radical Scavengers on Aerosol Formation from Reactions of β-Pinene with O 3, *Aerosol Sci. Technol.*, 2003, **37**, 877–891.

12 K. M. Henry, T. Lohaus and N. M. Donahue, Organic Aerosol Yields from α-Pinene Oxidation: Bridging the Gap between First-Generation Yields and Aging Chemistry, *Environ. Sci. Technol.*, 2012, **46**, 12347–12354.

13 E. Abramson, D. Imre, J. Beranek, J. Wilson and A. Zelenyuk, Experimental determination of chemical diffusion within secondary organic aerosol particles, *Phys. Chem. Chem. Phys.*, 2013, **15**, 2983–2991.

14 R. K. Pathak, K. Salo, E. U. Emanuelsson, C. Cai, A. Lutz, Å. M. Hallquist and M. Hallquist, Influence of Ozone and Radical Chemistry on Limonene Organic Aerosol Production and Thermal Characteristics, *Environ. Sci. Technol.*, 2012, **46**, 11660–11669.

15 M. S. Claflin, J. E. Krechmer, W. Hu, J. L. Jimenez and P. J. Ziemann, Functional Group Composition of Secondary Organic Aerosol Formed from Ozonolysis of α-Pinene Under High VOC and Autoxidation Conditions, *ACS Earth Space Chem.*, 2018, **2**, 1196–1210.

16 M. L. Walser, Y. Desyaterik, J. Laskin, A. Laskin and S. A. Nizkorodov, High-resolution mass spectrometric analysis of secondary organic aerosol produced by ozonation of limonene, *Phys. Chem. Chem. Phys.*, 2008, **10**, 1009–1022.

17 K. S. Docherty, W. Wu, Y. B. Lim and P. J. Ziemann, Contributions of Organic Peroxides to Secondary Aerosol Formed from Reactions of Monoterpenes with O3, *Environ. Sci. Technol.*, 2005, **39**, 4049–4059.

18 Y. Zhao, J. A. Thornton and H. O. T. Pye, Quantitative constraints on autoxidation and dimer formation from direct probing of monoterpene-derived peroxy radical chemistry, *Proc. Natl. Acad. Sci. U. S. A.*, 2018, **115**, 12142.

19 U. Molteni, M. Simon, M. Heinritzi, C. R. Hoyle, A.-K. Bernhammer, F. Bianchi, M. Breitenlechner, S. Brilke, A. Dias, J. Duplissy, C. Frege, H. Gordon, C. Heyn, T. Jokinen, A. Kürten, K. Lehtipalo, V. Makhmutov, T. Petäjä, S. M. Pieber, A. P. Praplan, S. Schobesberger, G. Steiner, Y. Stozhkov, A. Tomé, J. Tröstl, A. C. Wagner, R. Wagner, C. Williamson, C. Yan, U. Baltensperger, J. Curtius, N. M. Donahue, A. Hansel, J. Kirkby, M. Kulmala, D. R. Worsnop and J. Dommen, Formation of highly oxygenated organic molecules from α-pinene ozonolysis: chemical characteristics, mechanism, and kinetic model development, *ACS Earth Space Chem.*, 2019, **3**, 873–883.

20 C. M. Kenseth, Y. Huang, R. Zhao, N. F. Dalleska, J. C. Hethcox, B. M. Stoltz and J. H. Seinfeld, Synergistic O3 + OH oxidation pathway to extremely low-volatility dimers revealed in β-pinene secondary organic aerosol, *Proc. Natl. Acad. Sci. U. S. A.*, 2018, **115**, 8301.

21 R. R. Valiev, G. Hasan, V.-T. Salo, J. Kubečka and T. Kurten, Intersystem Crossings Drive Atmospheric Gas-Phase Dimer Formation, *J. Phys. Chem. A*, 2019, **123**, 6596–6604.

22 J. J. Orlando and G. S. Tyndall, Laboratory studies of organic peroxy radical chemistry: an overview with emphasis on recent issues of atmospheric significance, *Chem. Soc. Rev.*, 2012, **41**, 6294–6317.

23 F. Bianchi, J. Tröstl, H. Junninen, C. Frege, S. Henne, C. R. Hoyle, U. Molteni, E. Herrmann, A. Adamov, N. Bukowiecki, X. Chen, J. Duplissy, M. Gysel, M. Hutterli, J. Kangasluoma, J. Kontkanen, A. Kürten, H. E. Manninen, S. Münch, O. Peräkylä, T. Petäjä, L. Rondo, C. Williamson, E. Weingartner, J. Curtius, D. R. Worsnop, M. Kulmala, J. Dommen and U. Baltensperger, New particle formation in the free troposphere: a question of chemistry and timing, *Science*, 2016, **352**, 1109–1112.

24 J. Tröstl, W. K. Chuang, H. Gordon, M. Heinritzi, C. Yan, U. Molteni, L. Ahlm, C. Frege, F. Bianchi, R. Wagner, M. Simon, K. Lehtipalo, C. Williamson, J. S. Craven, J. Duplissy, A. Adamov, J. Almeida, A.-K. Bernhammer, M. Breitenlechner, S. Brilke, A. Dias, S. Ehrhart, R. C. Flagan, A. Franchin, C. Fuchs, R. Guida, M. Gysel, A. Hansel, C. R. Hoyle, T. Jokinen, H. Junninen, J. Kangasluoma, H. Keskinen, J. Kim, M. Krapf, A. Kürten, A. Laaksonen, M. Lawler, M. Leiminger, S. Mathot, O. Möhler, T. Nieminen, A. Onnela, T. Petäjä, F. M. Piel, P. Miettinen, M. P. Rissanen, L. Rondo, N. Sarnela, S. Schobesberger, K. Sengupta, M. Sipilä, J. N. Smith, G. Steiner, A. Tomè, A. Virtanen, A. C. Wagner, E. Weingartner, D. Wimmer, P. M. Winkler, P. Ye, K. S. Carslaw, J. Curtius, J. Dommen, J. Kirkby, M. Kulmala, I. Riipinen, D. R. Worsnop, N. M. Donahue and U. Baltensperger, The role of low-volatility organic

compounds in initial particle growth in the atmosphere, *Nature*, 2016, **533**, 527–531.

25 L. L. J. Quéléver, K. Kristensen, L. Normann Jensen, B. Rosati, R. Teiwes, K. R. Daellenbach, O. Peräkylä, P. Roldin, R. Bossi, H. B. Pedersen, M. Glasius, M. Bilde and M. Ehn, Effect of temperature on the formation of highly oxygenated organic molecules (HOMs) from alpha-pinene ozonolysis, *Atmos. Chem. Phys.*, 2019, **19**, 7609–7625.

26 T. Berndt, W. Scholz, B. Mentler, L. Fischer, H. Herrmann, M. Kulmala and A. Hansel, Accretion Product Formation from Self- and Cross-Reactions of RO2 Radicals in the Atmosphere, *Angew. Chem., Int. Ed.*, 2018, **57**, 3820–3824.

27 G. McFiggans, T. F. Mentel, J. Wildt, I. Pullinen, S. Kang, E. Kleist, S. Schmitt, M. Springer, R. Tillmann, C. Wu, D. Zhao, M. Hallquist, C. Faxon, M. Le Breton, Å. M. Hallquist, D. Simpson, R. Bergström, M. E. Jenkin, M. Ehn, J. A. Thornton, M. R. Alfarra, T. J. Bannan, C. J. Percival, M. Priestley, D. Topping and A. Kiendler-Scharr, Secondary organic aerosol reduced by mixture of atmospheric vapours, *Nature*, 2019, **565**, 587–593.

28 F. D. Lopez-Hilfiker, V. Pospisilova, W. Huang, M. Kalberer, C. Mohr, G. Stefenelli, J. A. Thornton, U. Baltensperger, A. S. H. Prevot and J. G. Slowik, An extractive electrospray ionization time-of-flight mass spectrometer (EESI-TOF) for online measurement of atmospheric aerosol particles, *Atmos. Meas. Tech.*, 2019, **12**, 4867–4886.

29 S. M. Platt, I. El Haddad, A. A. Zardini, M. Clairotte, C. Astorga, R. Wolf, J. G. Slowik, B. Temime-Roussel, N. Marchand, I. Ježek, L. Drinovec, G. Močnik, O. Möhler, R. Richter, P. Barmet, F. Bianchi, U. Baltensperger and A. S. H. Prévôt, Secondary organic aerosol formation from gasoline vehicle emissions in a new mobile environmental reaction chamber, *Atmos. Chem. Phys.*, 2013, **13**, 9141–9158.

30 A. Metzger, J. Dommen, K. Gaeggeler, J. Duplissy, A. S. H. Prevot, J. Kleffmann, Y. Elshorbany, A. Wisthaler and U. Baltensperger, Evaluation of 1,3,5 trimethylbenzene degradation in the detailed tropospheric chemistry mechanism, MCMv3.1, using environmental chamber data, *Atmos. Chem. Phys.*, 2008, 6453–6468.

31 V. Pospisilova, F. D. Lopez-Hilfiker, D. M. Bell, I. El Haddad, C. Mohr, W. Huang, L. Heikkinen, M. Xiao, J. Dommen, A. S. H. Prevot, U. Baltensperger and J. G. Slowik, On the fate of oxygenated organic molecules in atmospheric aerosol particles, *Sci. Adv.*, 2020, **6**, eaax8922.

32 L. Qi, M. Chen, G. Stefenelli, V. Pospisilova, Y. Tong, A. Bertrand, C. Hueglin, X. Ge, U. Baltensperger, A. S. H. Prévôt and J. G. Slowik, Organic aerosol source apportionment in Zurich using an extractive electrospray ionization time-of-flight mass spectrometer (EESI-TOF-MS) – Part 2: biomass burning influences in winter, *Atmos. Chem. Phys.*, 2019, **19**, 8037–8062.

33 G. Stefenelli, V. Pospisilova, F. D. Lopez-Hilfiker, K. R. Daellenbach, C. Hüglin, Y. Tong, U. Baltensperger, A. S. H. Prévôt and J. G. Slowik, Organic aerosol source apportionment in Zurich using an extractive electrospray ionization time-of-flight mass spectrometer (EESI-TOF-MS) – Part 1: Biogenic influences and day–night chemistry in summer, *Atmos. Chem. Phys.*, 2019, **19**, 14825–14848.

34 T. D. Vaden, D. Imre, J. Beranek, M. Shrivastava and A. Zelenyuk, Evaporation kinetics and phase of laboratory and ambient secondary organic aerosol, *Proc. Natl. Acad. Sci. U. S. A.*, 2011, **108**, 2190–2195.

35 G. M. Wolfe, M. R. Marvin, S. J. Roberts, K. R. Travis and J. Liao, The Framework for 0-D Atmospheric Modeling (F0AM) v3.1, *Geosci. Model Dev.*, 2016, **9**, 3309–3319.

36 M. E. Jenkin, S. M. Saunders, V. Wagner and M. J. Pilling, Protocol for the development of the Master Chemical Mechanism, MCM v3 (Part B): tropospheric degradation of aromatic volatile organic compounds, *Atmos. Chem. Phys.*, 2003, **3**, 181–193.

37 S. M. Saunders, M. E. Jenkin, R. G. Derwent and M. J. Pilling, Protocol for the development of the Master Chemical Mechanism, MCM v3 (Part A): tropospheric degradation of non-aromatic volatile organic compounds, *Atmos. Chem. Phys.*, 2003, **3**, 161–180.

38 M. E. Jenkin, S. M. Saunders and M. J. Pilling, The tropospheric degradation of volatile organic compounds: a protocol for mechanism development, *Atmos. Environ.*, 1997, **31**, 81–104.

39 M. R. McGillen, B. F. E. Curchod, R. Chhantyal-Pun, J. M. Beames, N. Watson, M. A. H. Khan, L. McMahon, D. E. Shallcross and A. J. Orr-Ewing, Criegee Intermediate–Alcohol Reactions, A Potential Source of Functionalized Hydroperoxides in the Atmosphere, *ACS Earth Space Chem.*, 2017, **1**, 664–672.

40 H. J. Tobias and P. J. Ziemann, Kinetics of the Gas-Phase Reactions of Alcohols, Aldehydes, Carboxylic Acids, and Water with the C13 Stabilized Criegee Intermediate Formed from Ozonolysis of 1-Tetradecene, *J. Phys. Chem. A*, 2001, **105**, 6129–6135.

41 S. M. Aschmann, A. A. Chew, J. Arey and R. Atkinson, Products of the Gas-Phase Reaction of OH Radicals with Cyclohexane: Reactions of the Cyclohexoxy Radical, *J. Phys. Chem. A*, 1997, **101**, 8042–8048.

42 M. Schervish and N. M. Donahue, Peroxy radical kinetics and new particle formation, *Environ. Sci.: Atmos.*, 2021, **1**, 79–92.

43 M. Schervish and N. M. Donahue, Peroxy radical chemistry and the volatility basis set, *Atmos. Chem. Phys.*, 2020, **20**, 1183–1199.

44 J. Zhou, E. A. Bruns, P. Zotter, G. Stefenelli, A. S. H. Prévôt, U. Baltensperger, I. El-Haddad and J. Dommen, Development, characterization and first deployment of an improved online reactive oxygen species analyzer, *Atmos. Meas. Tech.*, 2018, **11**, 65–80.